

Fragility Curves Derivation for a Pile-Supported Wharf

H. Heidary Torkamani*, K. Bargi, R. Amirabadi

*Civil Engineering Department, School of Civil Engineering, College of Engineering, University of Tehran, Tehran, Iran; hamid_heidary@ut.ac.ir.

ARTICLE INFO

Article History:

Received: 30 September 2012

Accepted: 27 April 2013

Available online: 30 June 2013

Keywords:

Fragility Curve

Incremental Dynamic Analysis

Pile-Supported Wharves

Seismic Vulnerability

ABSTRACT

This study aims to develop seismic fragility curves for a typical pile-supported wharf. Fragility curve is one of the popular tools in seismic performance evaluation of a structure. The software FLAC2D was used to simulate the seismic performance of the wharf structure. Using eight time history records, occurred in past, as seismic loading, incremental dynamic analysis (IDA) was applied for seismic demand estimation. Based on the resulted seismic response matrix the analytical fragility curves were developed. As a prevailing tool, adopted fragility curves are useful for seismic risk assessment. They can also be used to optimize wharf-retrofit methods.

1-Introduction

During past decades, a number of pile-supported wharves suffered extensive earthquake induced damages due to poor seismic design [1]. As seaports play a significant role in the world's economy, their seismic performance should be enhanced. Therefore, it is necessary to assess seismic performance of port facilities under different levels of seismic loadings. Pile-supported wharf structures are one of the most common types of berthing facilities in seaports, and seismically induced damages in past events have shown the necessity of enhancement of the seismic performance of this type of structures. Seismic fragility analysis is a simple but powerful tool for evaluating the seismic vulnerability of a structural system. The input to the analysis is the ground motion intensity measure (IM) and the output is the probability of exceeding a specific damage state. Over the last few years, fragility approach was commonly developed for a great variety of structural systems, such as RC frame/wall systems, RC structural walls, steel frames and RC bridges [2-7], caisson quay walls and pile-supported wharf structures on steel vertical piles [2, 8]. Although many researches were made to investigate the seismic performance of wharf structures under seismic loading [9, 10], less effort is done on seismic vulnerability assessment of wharf structures. Considering this, in the present paper, a new methodology for developing fragility curves for typical pile-supported wharves is proposed. Fragility information is expressed as a relationship between the severity of ground motion and the probability of reaching or exceeding different damage levels. The

most common two formats for the fragility analysis output are damage probability matrix and fragility curves. The damage probability matrix gives the probability of different damage states at a specific level of ground motion, while each fragility curve gives the probability of a specific damage state at different levels of ground motion. Fragility curves can be developed for one specific system or for a class of systems. Based on the method used to generate them, fragility curves are classified as either analytical or empirical [11, 12]. Analytical fragility curves are generated using results of numerical simulations of the system under artificial or historical earthquake records. Empirical fragility curves are based on experimental results or damage data collected from the field after earthquakes. In some cases, opinion of experts and personal judgment can be the basis for empirical fragility curves [11]. The main challenges for analytical methods are generating artificial ground motions that are consistent with the site specification and relating numerical results of the simulation to predefined levels of damage. Scarcity of available data is the main deficiency of the empirical methods. Fragility information describes the potential of structures to be damaged under earthquakes. Since it does not reflect the seismic hazard at the site of the structure, fragility information is not enough by itself to estimate the seismic risk or to give estimates for expected losses due to earthquakes. Only when integrated with seismic hazard and cost data, fragility information can provide estimates for the seismic risk [11-13].

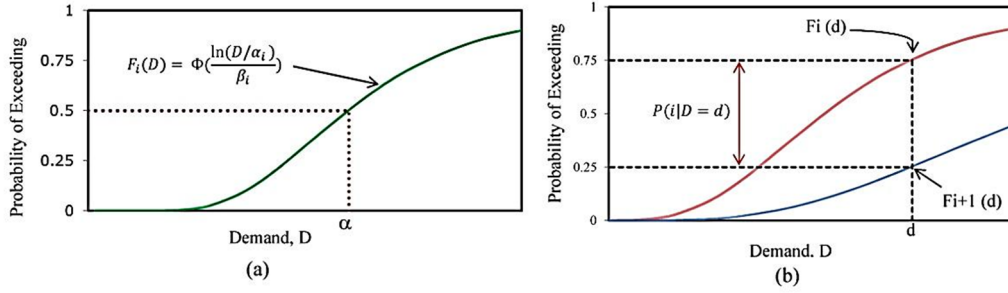


Figure 1. a) Fragility function definition b)Evaluating individual damage-state probabilities [12]

2. Fragility Definition

In general, fragility functions are probability distributions that indicate the probability that a structural system or component will be damaged to a predefined damage state as a function of an engineering demand parameter (EDP) such as displacement ductility factor (μ_d). Herein, fragility functions take the form of lognormal cumulative distribution functions, having a median value α and logarithmic standard deviation, β [11]. The mathematical form for such a fragility function is:

$$F_i(D) = \Phi\left(\frac{\ln(D / \alpha_i)}{\beta_i}\right) \tag{1}$$

Where;

$F_i(D)$: is the conditional probability that the structural component may be damaged to damage state “i” as a function of demand parameter, “D”.

$\Phi(\cdot)$: is the standard normal cumulative distribution function.

α_i : is the median value of the probability distribution.

β_i : is the logarithmic standard deviation.

The probability that a structural element or system may be damaged to damage state “i” and not to a more or less severe level given that it experiences demand, D is provided by Eq. (2):

$$P(i|D) = F_i(D) - F_{i+1}(D) \tag{2}$$

Where;

$F_{i+1}(D)$ is the conditional probability that the component will be damaged to damage state “i+1” or a more severe state.

$F_i(D)$ is as similarly defined. Figure 1 illustrates the definition of Eq. (2).

Fragility analysis is based on correlating damage data with the severity of the corresponding ground motions. There are main four sources for the data upon which fragility information is based, including

actual damage data collected from the field after past earthquakes, test results, numerical simulation results, and engineering judgment. The following is a brief description of each of these sources with some examples.

2.1. Field damage data

In this approach, the damage data used in fragility analysis is obtained from field damage observations after earthquakes. One of the challenges in this case is estimating the spatial distribution of the earthquake intensity and getting the value of this intensity at each location for the structures. Another challenge is to define the damage state at every location based on merely visual examination [11]. Sometimes the damage data comes from different resources with different ground motion intensity parameters and damage states. Transforming the data from one format to another is another challenge with this method. Also, the scarcity and lack of accuracy in such data make it very difficult to develop comprehensive and accurate fragility information. An example of fragility curves developed using damage data associated with past earthquakes is the work of Shinozuka *et al.* [14]. Two families of empirical fragility curves were developed utilizing bridge damage data.

2.2. Test results damage data

In this approach, a series of tests is considered to generate damage data that can be used in fragility analysis. The advantage of this approach is having full control over the range of ground motion excitation and the ability to accurately measure the damage in the considered structure. However, this approach is very expensive and limited by the capacity of the available shaking table and other testing equipment. Also, testing is always time-consuming. An example of this approach is the work of Chong *et al.* [15] where fragility curves were developed for a free-standing rigid block based on experimental data.

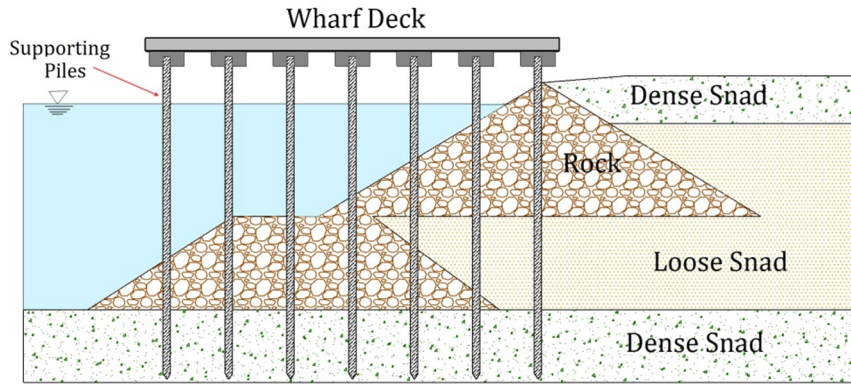


Figure 2. Cross section profile of the selected wharf showing structural elements and soil layers

2.3. Numerical simulation approach

In principal, this approach is similar to the experimental approach except that it replaces testing with numerical analysis to obtain damage data. The structure is analyzed under different seismic excitations with different intensities. There are two approaches for generating seismic excitations used in the analysis. The first approach is using acceleration time histories of past earthquakes after scaling them to the desired intensities. The second approach is to generate artificial seismic excitations based on theoretical stochastic models. The structure is modeled and analyzed under each realization and the damage state is estimated based on the analysis results. An example of fragility curves based on detailed nonlinear dynamic analysis is the work of Mostafa *et al.*[16]. Fragility curves have been developed for a water tank on top of a hospital in New York City.

2.4. Engineering judgment approach

In this approach, the damage states are defined in a quantitative format and experts and professionals develop estimates of the damage expected from ground motions of different intensities. This approach is less costly than the previous approaches and takes less time. However it is far less accurate and subjected to personal judgment. It is highly preferable when fragility curves are to be developed for a wide range of structures and damage states. This approach was adopted by FEMA in its methodology for earthquake loss estimation called HAZUS[17]. For fragility curves derivation, at first the ground motions and their representative intensity measure, wharf structure and seismic performance indicator of wharf should be determined. The following sections describe the fragility curve derivation requirements. Due to the lack of damage data from past events in the case of pile supported-wharves, in present study, the numerical simulation approach is used.

3. Ground Motion Records and Wharf Characterization

To evaluate the engineering seismic demand (EDP) values (here displacement ductility factor) of wharf

structure and their associated uncertainties at a particular site, records are better obtained from stations with similar geologic conditions to that site. The number of ground motions should be sufficient to yield response quantity statistics. In addition, the selected ground motion records should capture the characteristics of the possible seismic hazards[18]. Under the above considerations, in present paper, an ensemble of eight earthquake records were obtained from the PEER Strong Motion Database[19]. Their basic information and properties are shown in table 1.

Table 1. Details of the ground motion records used in this study [19]

No.	Event	Year	Magnitude	R(km)	PGA(g)
1	Imperial Valley	1979	7	28.7	0.27
2	Imperial Valley	1979	7	43.6	0.351
3	Livermore	1980	6	17.6	0.154
4	Loma Prieta	1989	7	57.4	0.171
5	Loma Prieta	1989	7	36.3	0.278
6	Loma-Prieta	1989	7	28.8	0.209
7	Morgan Hill	1984	6	38.1	0.142
8	Northridge	1994	7	13	0.482

To illustrate the fragility analysis for pile-supported wharf structures, the centrifuge model NJM01 as a typical pile-supported wharf structure was selected [9]. This centrifuge model was conducted at the geotechnical modeling center of California University, (UC Davis) to evaluate seismic performance of pile-supported wharf structures. The chosen configuration for the tests is generalized representation of typical pile-supported wharf structures from western United States ports.

Figure 2 shows the cross-section profile of the wharf model.

In present paper, the structural properties (e.g. properties of deck and piles) and geotechnical parameters of different soil layers are defined according to NJM01 model provided by McCullough [9].

Table 2 and Table 3 shows the geometrical and structural properties of wharf. In addition, the geotechnical parameters of soil layers are provided in Table 4. More detailed information can be easily found in [9].

Table 2. Summary of the wharf model in prototype scale [22]

Water Depth (m)	Rock Dike Height (m)	Transverse Pile Spacing (m)	Longitudinal Pile Spacing (m)
16	19.5	5.1	6.1

Table 3. Piles and deck properties of the wharf [22]

Structural Properties	Values in prototype scale
Pile Diameter (mm)	636
Pile Wall Thickness (mm)	50.8
Pile Moment of Inertia (m ⁴)	3.02 × 10 ⁻³
Modulus of Elasticity (GPa)	70
Plastic Moment (N-m)	7.5 × 10 ⁶
Wharf Deck Thickness (mm)	255

Table 4. Geotechnical parameters of different soil layers [22]

Type of Soil	Soil Characteristics	Value
Loose Sand	Relative Density (%)	39
	Dry Mass Density (kg/m ³)	1519
	Porosity (%)	43.4
	Friction Angle (deg)	33
	Dilation Angle (deg)	6.6
Dense Sand	Relative Density (%)	82
	Dry Mass Density (kg/m ³)	1662
	Porosity (%)	39.11
	Friction Angle (deg)	37.91
Rock Fill	Dilation Angle (deg)	24.3
	Dry Mass Density (kg/m ³)	1682
	Porosity (%)	37.7
	Friction Angle (deg)	45
	Dilation Angle (deg)	15

4. Finite Difference Modeling

In order to simulate seismic performance of the pile-supported wharf, a two-dimensional (2D) nonlinear finite difference model (

Figure 3) was constructed using the software FLAC2D (Fast Lagrangian Analysis of Continua) [20].

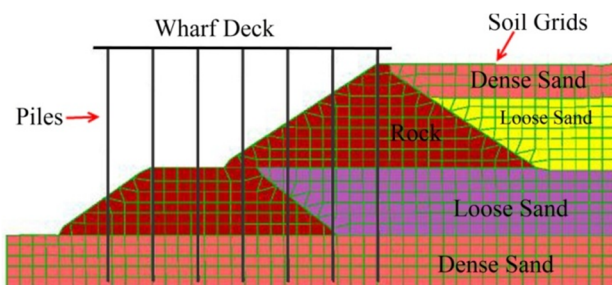


Figure 3. Finite difference model of the wharf

This software is a 2D explicit finite difference computer program and widely used for the simulation of seismic performance of port structures and soil-structure interaction (SSI) analysis under static and seismic loading conditions by many previous researchers [8, 21-23].

In order to model piles, the pile option was selected with an interface element for modeling soil-structure interaction (SSI). The interface element uses springs to model the shear and normal SSI behavior [20]. Normal and shear interface elements are analogous to p-y and t-z springs, respectively, that are commonly used in the lateral and vertical analyses of piles. The piles were modeled as non-linear elements having a bi-linear moment-curvature relationship.

The wharf deck was modeled using beam element. Due to large thickness of deck and corresponding substantial rigidity in the horizontal plane, flexural deformations of the deck are negligibly small. Therefore, the deck was idealized as an elastic beam.

Regarding static solutions, the bottom boundary is fixed in the horizontal and vertical directions and lateral boundaries in the horizontal direction. For dynamic solutions, the free-field boundary conditions are presumed to simulate lateral boundaries.

It should be noted that FLAC 2D offers the free-field boundary condition and damping property for the seismic analysis [20].

An effective stress Mohr-Coulomb constitutive model was used as constitutive soil model. For liquefaction susceptible soils the modified equation of Martin [24], presented by Byrne [25], was used to model pore pressure generation.

The elastic soil behavior was defined by bulk and shear modulus values of soil, soil strength by effective angle of friction and cohesion, and volumetric shear behaviour by a dilation angle [20].

Based on [22] a dilation angle of zero degree, an artificial cohesion of 15 kPa for the rock, and a reduction in down slope spring stiffness by a factor of 10 were used. In this paper, water located above the ground surface was modeled as normal pressure acting on the soil surface. The water within the soil was modeled as incompressible, with steady state, hydrostatic pore pressures and the potential for the generation of excess pore pressures in liquefiable soils. Groundwater flow was not modeled in the dynamic analyses. This simplification shows proper compatibility with other modeling hypotheses and the analysis time of models has been reduced as well. Pore pressures were generated during dynamic loading but not dissipated. The mentioned simplification was justified since minimal pore pressure dissipation was expected during the relatively short application of earthquake shaking (10 to 30 seconds).

The damping for soil and structural elements were 5% and 1%, respectively.

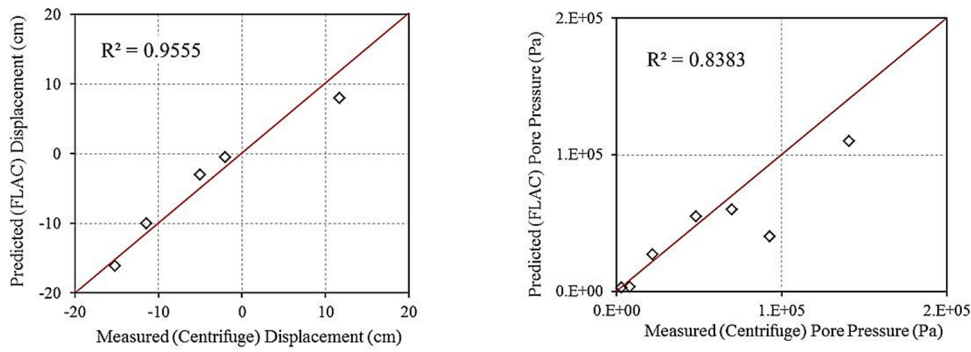


Figure 4. Verification analyses results

5. Analyses Procedure

Three different analyses were performed; 1) Validation analysis for calibrating the input data and verifying the output data with centrifuge tests results; 2) Static pushover analysis for obtaining yield values; 3) Dynamic time-history analysis for seismic demand values (here displacement ductility factor) determination.

5.1. Validation analysis

In order to verify the numerical model, the model was subjected to the Loma Prieta earthquake (1989) time history, recorded at the Oakland Outer Harbor and the results predicted by the FLAC model were compared with the measured data of the centrifuge model adopted from [22]. The results of the validation analysis are presented in

Figure 4. In this figure, the vertical axis shows the values predicted by the FLAC numerical model while the horizontal axis indicates the data obtained from the centrifuge data [22]. Ideally, all scatter data should lie on the $y=x$ line as shown in red line.

In order to quantitatively assess the performance of the numerical model, the coefficient of correlation (R^2) was used. This parameter is calculated using Eq.(3) and are shown in Figure 4.

$$R^2 = \frac{\sum(x_i - \bar{x})(y_i - \bar{y})}{\sqrt{\sum(x_i - \bar{x})^2 \sum(y_i - \bar{y})^2}} \quad (3)$$

where y_i stands for the measured value from the centrifuge model, x_i denotes the predicted value resulted from the FLAC model, \bar{y} and \bar{x} represents the mean of y values and x values, respectively.

Given the values of the R^2 , it can be concluded that the predicted values are generally close to the measured values. This indicates that the FLAC numerical model used in this study captures well the seismic performance of wharf under study. In other words, the numerical model is valid enough to simulate the seismic performance of the pile-supported wharf for further fragility analysis.

5.2. Static analysis

A pushover analysis was performed in order to evaluate the yield and ultimate values of the wharf structure. The yield lateral force value (f_y) was determined as the break-point in the pushover curve. Accordingly, the yield displacement (d_y), denotes the displacement corresponding to the wharf structure yield. Ultimate lateral force value (f_u) is determined as the point at which the double plastic hinges is occurred in the initial pile. The yield lateral displacement (d_y), yield lateral force (f_y), ultimate lateral displacement (d_u), and f_u were presented in Table 5.

Table 5. Pushover analysis results

d_y (m)	f_y (kN)	d_u (m)	f_u (kN)
0.23	3040	1.56	4331

5.3. Seismic demand estimation

Incremental Dynamic Analysis (IDA) is applied to assess the seismic response of the wharf structure. IDA, proposed by Vamvatsikos and Cornell[26] is a computational-based methodology to estimate structural performance under different levels of seismic loading.

The IDA approach involves performing nonlinear dynamic analyses to a structure under a suite of ground motion records; each scaled to several intensity levels. Herein, the spectral acceleration at the natural period of the wharf structure (i.e. $S_a(T_n)$) is selected as the intensity measure (IM) used to describe ground motion characteristics. The first reason behind this selection is that seismic demand estimates are strongly correlated with the linear-elastic spectral response acceleration at the natural period of the structure (T_n)[18]. Moreover, based on four criteria (i.e. practicality, sufficiency, effectiveness and efficiency) Amirabadi *et al.*[27] showed that $S_a(T_n)$ is the optimal IM for seismic performance assessment of pile-supported wharf structures.

In order to perform IDA, S_a is incrementally increased from 0.2 (m/sec^2) to 15 (m/sec^2) using stepping algorithm. The final S_a levels are shown in Table 6.

A set of incremental time history analyses was performed by applying scaled accelerograms and displacement ductility values (μ_d) were monitored during each analysis.

Displacement ductility factor (μ_d) is the ratio of maximum relative horizontal displacement (between the bottom and top of the pile) to the horizontal displacement at the yielding state derived from pushover analysis.

According to the concept of IDA, given a time history record each dynamic analysis at a certain S_a level, provides a value of the selected EDP as an scatter point in Figure 5. In this figure the mean value of all

resulted demand quantities (i.e. mean IDA curve) is shown.

6. Derivation of Analytical Fragility Curves

Having the wharf seismic response quantities, fragility analysis can be performed within three steps. The first step is introducing proper quantitative damage states. The second is performing statistical analysis to deduce the fragility curves. The final step is to simplify the obtained fragility curves for easy further application. Each step is described as following.

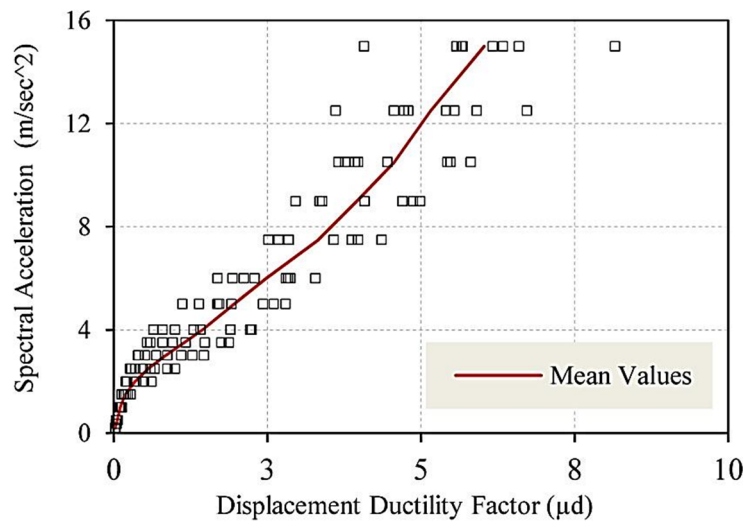


Figure 5. Seismic response values and mean IDA curve of the wharf

Table 6. Seismic response matrix of the wharf under study resulted from IDA

Spectral Acceleration (m/s ²)	Displacement Ductility Factor (μ_d)							
	Event #1	Event #2	Event #3	Event #4	Event #5	Event #6	Event #7	Event #8
0.2	0.02	0.03	0.02	0.02	0.03	0.02	0.02	0.02
0.35	0.04	0.04	0.03	0.03	0.04	0.04	0.03	0.04
0.5	0.06	0.06	0.05	0.05	0.06	0.05	0.04	0.05
1.0	0.11	0.13	0.09	0.09	0.11	0.09	0.11	0.11
1.5	0.16	0.22	0.13	0.19	0.16	0.13	0.27	0.19
2.0	0.32	0.37	0.20	0.37	0.19	0.21	0.61	0.49
2.5	0.47	0.59	0.29	0.66	0.26	0.35	1.00	0.87
3.0	0.69	0.87	0.39	1.09	0.40	0.50	1.46	1.28
3.5	0.95	1.17	0.59	1.47	0.54	0.79	1.87	1.74
4.0	1.29	1.41	0.79	1.90	0.64	0.99	2.22	2.24
5.0	1.72	1.92	1.38	2.43	1.11	1.69	2.79	2.60
6.0	2.11	2.29	1.93	2.87	1.69	2.80	3.28	2.84
7.5	2.84	2.84	2.68	3.87	2.51	3.57	4.35	3.97
9.0	3.39	2.95	3.35	4.69	3.35	4.08	4.87	4.98
10.5	3.92	3.65	3.97	5.43	3.76	4.45	5.48	5.81
12.5	4.56	3.61	4.72	6.72	4.79	5.41	5.54	5.90
15.0	5.66	4.07	5.58	8.15	5.67	6.33	6.17	6.59

Table 7. Bounds of damage states for the wharf under study[28]

	Damage state		
	Degree I ,Serviceable	Degree II, Repairable	Degree III, Near collapse
Piles (peak response)	Essentially elastic response with minor or no residual deformation	Controlled limited inelastic ductile response and residual deformation intending to keep the structure repairable.	Ductile response near collapse (double plastic hinges may occur at one or limited number of piles)
Displacement ductility factor value	1	3.89	6.78

6.1. Damage states

For the purpose of fragility analysis, three different damage states were defined in term of displacement ductility factor (μ_d), following qualitative criteria for judging the degree of damage to a pile- supported wharf based on the peak responses of the piles presented at PIANC [28]. The description and values are displayed in the Table 6.

Based on the sequence of plasticity development in the pushover process, for a pile-supported wharf structure, serviceability is essentially elastic response with minor or no residual deformation. Therefore, serviceability is violated at $\mu_d = 1$ where the displacement of a wharf structure exceeds the displacement value corresponding to the structure yield point (d_y), derived from the pushover analysis.

Based on the definition of the PIANC (as shown in Table 6), a near-collapse limit state is reached when double plastic hinges occur at only one or a limited number of the piles. Herein, a near collapse limit state refers to the point in which double plastic hinges occur at the initial pile. This point is defined as “ultimate point” in the pushover process presented in Section 5.2. Therefore, the bound of a near collapse state in term of the μ_d value is defined as the ratio between ultimate displacement (d_u) and yield displacement (d_y). Hence, the μ_d value of a near

collapse limit state is equal to $6.78 \left(= \frac{d_u}{d_y} = \frac{1.56}{0.23} \right)$.

Reparability is a state in which a wharf structure has controlled inelastic ductile response and limited residual deformation, keeping the structure repairable. In order to define a bound for the reparability state, the average value of μ_d for the near collapse and serviceability limit states are used. Thus, the bound of reparability state is estimate to be

$$3.89 \left(= \frac{\mu_{d,yield} + \mu_{d,ultimate}}{2} = \frac{1 + 6.78}{2} \right).$$

In summary, the bound of μ_d corresponding to the serviceability, near collapse and reparability states are defined as $\mu_{d,yield} = 1$, $\mu_{d,ultimate} = 6.78$ and the yield-ultimate average value, respectively, as shown in table 7.

6.2. Fragility analysis

For each S_a level, the displacement ductility factor values can be further assumed to be a lognormal distribution with the probability density function (PDF) as follows [11]:

$$F_x(X) = \frac{1}{\sqrt{2\pi}\xi x} * \exp \left[-\frac{1}{2} \left(\frac{\ln x - \alpha}{\beta} \right)^2 \right] \quad (4)$$

$$0 \leq X < \infty$$

In which α and β are the two parameters of the lognormal distribution of the random displacement variable X . They can be calculated from the information on the two parameters of the normal distribution, the mean (μ) and the standard deviation (σ) of the sample population as shown below:

$$\alpha = \ln \mu - \frac{1}{2} \beta^2 \quad (5)$$

$$\beta = \sqrt{\ln \left[1 + \left(\frac{\sigma}{\mu} \right)^2 \right]} \quad (6)$$

According to the displacement ductility factor bounds of each defined damage states, the fragility curve for the damage state D_i is the conditional probability that the wharf has a state of damage exceeding the damage state D_i at a specific S_a level, as shown below:

$$[D > d | S_a] = P [X > x_i | S_a] = 1 - \Phi \left[\frac{\ln(x_i) - \alpha}{\beta} \right] \quad (7)$$

In which $\Phi(\cdot)$ is the standard normal cumulative distribution function, x_i is the upper bound for each damage states (I -serviceable, II-repairable, III- Near collapse), and α and β are as defined above. In this way, the fragility curves can be obtained as shown in Figure 6. The calculated parameter for each earthquake event (table 1) is shown in table 8.

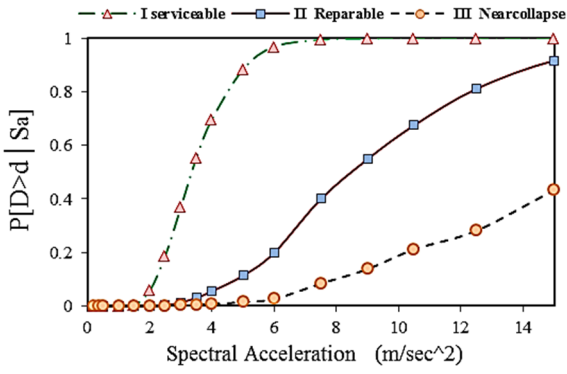


Figure 6. Fragility curve of the wharf under study

Table 8. Lognormal distribution parameters of the wharf under study

Spectral Acceleration (m/s ²)	μ	σ	α	β
0.2	0.02	0.00	-3.77	0.21
0.35	0.04	0.01	-3.22	0.21
0.5	0.06	0.01	-2.88	0.18
1.0	0.12	0.04	-2.19	0.36
1.5	0.22	0.14	-1.70	0.58
2.0	0.42	0.34	-1.12	0.71
2.5	0.69	0.57	-0.64	0.72
3.0	1.02	0.83	-0.24	0.72
3.5	1.38	1.04	0.09	0.67
4.0	1.71	1.22	0.33	0.64
5.0	2.30	1.41	0.67	0.57
6.0	2.89	1.55	0.93	0.50
7.5	3.87	2.03	1.23	0.49
9.0	4.57	2.21	1.41	0.46
10.5	5.24	2.44	1.56	0.44
12.5	5.85	2.31	1.69	0.38
15.0	6.80	2.51	1.85	0.36

6.3. Simplified fragility curves

As a common practice, the fragility curves are usually expressed as lognormal cumulative distribution functions (lognormal CDF). This section describes the idea used to fit the fragility curves to the lognormal cumulative distribution function and generating simplified fragility curves.

In this way, the fragility curves can be represented by only two parameters, as follows:

$$F_A(a) = \int_0^a \frac{1}{\sqrt{2\pi}\zeta_A(a)} \times \exp\left[-\frac{1}{2}\left(\frac{\ln(a)-\ln(m_A)}{\zeta_A}\right)^2\right] da \tag{8}$$

where A is the random variable of the S_a , m_A is the median of A , and ζ_A is the logarithmic standard deviation of A .

On the fragility curve, for the fragility probability $F_A(a)$ at a S_a level of “a”, the associated normal variable can be computed using the following equation:

$$Z = \Phi^{-1}\left[F_A(a)\right] \tag{9}$$

where $\Phi^{-1}(\cdot)$ is the inverse function of the standard normal cumulative distribution. Z is the standard normal variable, which is defined as Eq.(10).

$$Z = \frac{\ln(a)-\ln(m_A)}{\zeta_A} \tag{10}$$

Considering above approach, in order to generating simplified fragility curves, at first, for each fragility curve, the standard normal variables Z associated with the fragility probabilities for all S_a levels are calculated using Eq. (10). Then, the relationship of the standard normal variable Z versus the associated $\ln(a)$ value is constructed to retrieve the values of $\ln(m_A)$ and ζ_A . The simplified curves are displayed in Figure 7.

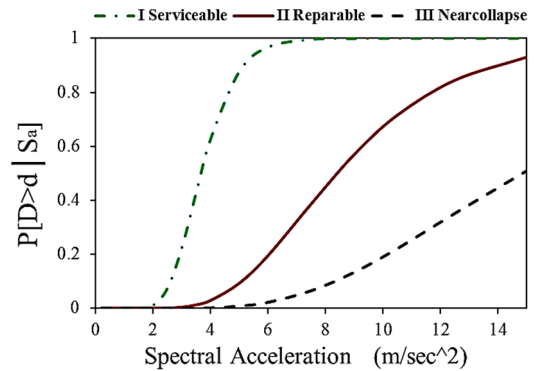


Figure 7. Simplified fragility curves

7. Conclusion

In this study a feasible procedure was proposed for developing seismic fragility curves of a typical pile-supported wharf. Fragility curves were developed using the spectral acceleration ($S_a(T_n)$) as IM and displacement ductility factor (μ_d) as engineering demand parameter (EDP).

From the resulted fragility curves, it is easy to read the damage probability for each damage state at a specific S_a level. For example, as shown in

Figure 8, when the S_a is at $0.6g = 6(m/s^2)$, the fragility probabilities for the damage states I, II and III are 97%, 20% and 3%, respectively.

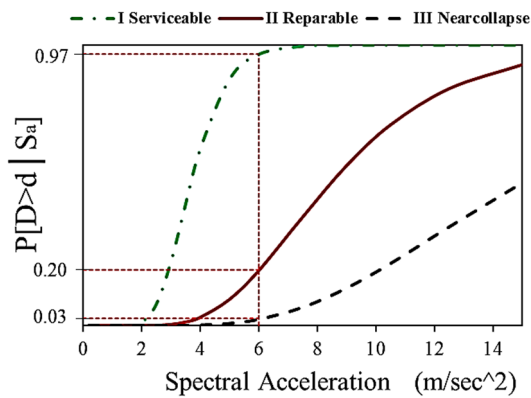


Figure 8. Simplified fragility curves with damage probabilities at $S_a=0.6g$

Presenting appropriate quantitative damage states in term of displacement ductility factor is a key issue in fragility analysis. In this study, three damage states including serviceability, reparability and near-collapse were considered and the bounds of each damage state in term of displacement ductility factor were quantified based on the PIANC qualitative description.

It should be noted that any other choice of IM-EDP pairs for fragility analysis will make the resulted fragility curves different and it is informative to compare fragility curves based on other IM-EDP pairs. One of the most popular EDP in fragility analysis is peak ground acceleration (PGA) which was used frequently for fragility analysis of bridges [5] and also pile-supported wharves [29] and gravity type quay walls [17].

In summary, the proposed framework for fragility derivation has a great potential for more future development.

The resulted fragility curves can be applied for many purposes such as seismic risk assessment and a real-time seismic damage assessment. Having the fragility curves, it is easy to determine the relationship between earthquakes induced loss and the input intensity level. The probability of each damage state given by fragility curve gives the estimated loss for each input excitation level. In more clear words, seismic risk assessment is enabled by the proposed fragility curves.

Moreover, the information gained by a seismic fragility analysis would be helpful in choosing optimal seismic retrofit methods for wharf structures.

8. References

- 1-Werner, S.D., (1998), *Seismic guidelines for ports*, Monograph No. 12, New York, ASCE.
- 2-Nielson, B. and DesRoches, R., (2007), *Analytical seismic fragility curves for typical bridges in the central and southeastern United States*, Earthquake Spectra, Vol.23(3), p. 615-33.
- 3-Hwang, H., Jernigan, J. and Lin, Y., (2000), *Evaluation of seismic damage to Memphis bridges and*

highway systems, Journal of Bridge Engineering, Vol. 5(4): p. 322-30.

4-Kwon, O. and Elnashai, A., (2010), *Fragility analysis of a highway over-crossing bridge with consideration of soil-structure interaction*, Structural and Infrastructural Engineering, Vol. 6(1): p. 59-78.

5-Tavares, D.H., Padgett, J.E., and Paultre, P., (2012), *Fragility curves of typical as-built highway bridges in eastern Canada*, Engineering Structures, Vol. 40: p. 107-118.

6-Nielson, B. and DesRoches, R., (2007), *Seismic fragility methodology for highway bridges using a component level approach*, Earthquake Engineering and Structural Dynamics. Vol. 36: p. 823-39.

7-Pan, Y., et al., (2010), *Seismic fragility of multispan simply supported steel highway bridges in New York state Part I: bridge modeling, parametric analysis and retrofit design*, Journal of Bridge Engineering. Vol. 15(5): p. 448-61.

8-Na, U.J., Chaudhuri, S.R., and Shinozuka, M., (2008), *Probabilistic assessment for seismic performance of port structures*, Soil Dynamics and Earthquake Engineering, Vol. 28(2): p. 147-158.

9-McCullough, N.J., et al., (2007), *Centrifuge seismic modeling of pile-supported wharves*, Geotechnical Testing Journal, Vol. 30(5): p. 349-59.

10-Chang, W.J., et al., (2010), *In situ dynamic model test for pile-supported wharf in liquefied sand*, Geotechnical Testing Journal, Vol. 33(3): p. 212-224.

11-Shinozuka, M., et al., (2000), *Statistical analysis of fragility curves*, Journal of Engineering Mechanics. Vol. 126(12): p. 1224-31.

12-Porter, K., Hamburger, R., and Kennedy, R., (2007), *Practical Development and Application of Fragility Functions*, Proc. of SEI Structures Congress, Long Beach CA, America.

13-Mander, J. and Basöz, N., (1999), *Seismic fragility curve theory for highway bridges*, Tech Council Lifeline Earthq Eng Monograph. Vol. 16: p. 31-40.

14-T. Nakamura, T.N., T. Shizuma and M. Shinozuka, (1998), *A study on failure probability of highway bridges by earthquake based on statistical method*, Proc of the 10th Japanese Earthquake Engineering Symposium.

15-Chong, W.H., & Soong, T. T., (2000), *Sliding fragility of unrestrained equipment in critical facilities*, Technical Report MCEER.

16-MOSTAFA, E.M., (1997), *Fragility curves for non-structural systems*, Earthquake Loss Methodology. HAZUS Technical Manual.

17-FEMA. *HAZUS 99 estimated annualized earthquake losses for the United States*, FEMA 366, S.

18-Shome, N., et al., (1998), *Earthquakes, records, and nonlinear responses*, Earthquake Spectra. Vol. 14(3): p. 467-500.

- 19-
http://peer.berkeley.edu/peer_ground_motion_database
- 20-Itasca, *Itasca Consulting Group, Minneapolis, MN*, in *FLAC version 4 User's Manual 2000*.
- 21-Boland, J.C., et al., (2001), *The seismic performance of a pile supported wharf centrifuge data and report for test(JCB01)*, DATA REPORT GEG05-2000.
- 22-McCullough, N.J., *The seismic geotechnical modeling, performance, and analysis of pile-supported wharves*, Oregon State University, Corvallis, OR, 2003.
- 23-Na, U.J., Chaudhuri, S.R. and Shinozuka, M., (2009), *Effects of spatial variation of soil properties on seismic performance of port structures*. *Soil Dynamics and Earthquake Engineering*. Vol. 29: p. 537-45.
- 24-Martin, G.R., Finn, W.D.L. and B., S.H., (1975), *Fundamentals of Liquefaction under Cyclic Loading*, *Journal of Geotechnical and Geoenvironmental Engineering*. Vol. 101(GT5): p. 423-438.
- 25-Byrne, P.A., (1991), *Cyclic Shear-Volume Coupling and Pore-Pressure Model for Sand In Proceedings: Second International Conference on Recent Advances in Geotechnical Earthquake Engineering and Soil Dynamics* (St. Louis, Missouri, March). Vol. 24(1): p. 47-55.
- 26-Vamvatsikos, D. and Cornell, C.A., (2002), *Incremental dynamic analysis*. *Earthquake Engineering and Structural Dynamic*, Vol. 31: p. 491-514.
- 27-Amirabadi, R., Bargi, K. and Heidary Torkamani, H., (2012), *Seismic Demands for Pile-Supported Wharf Structures with Batter Piles*, *Research Journal of Applied Sciences, Engineering and Technology*, Vol. 4(19): p. 3791-3800.
- 28-*Seismic design guidelines for port structures*, in *International Navigation Association (PIANC)2001*, A.A.Balkema.
- 29-Na, U.J., Chaudhuri, S.R. and Shinozuka, M., (2009), *Performance evaluation of pilesupported wharf under seismic loading*, *Proc., TCLEE 2009: Lifeline Earthquake Engineering in a Multihazard Environment*: p. 1032-1041.